Wear, 55 (1979) 221 - 234

CAVITATION EROSION OF ALUMINUM CONSIDERING BUBBLE COLLAPSE, PULSE HEIGHT SPECTRA AND CAVITATION EROSION EFFICIENCY*

F. G. HAMMITT and M. K. DE

Mechanical Engineering Department and Nuclear Engineering Department, University of Michigan, Ann Arbor, Michigan (U.S.A.)

(Received October 23, 1978)

Summary

Water erosion data on 1100-0 aluminum specimens obtained using a cavitating venturi are compared with bubble collapse pulse height spectra measured using a microtransducer. The data are resolved into erosion power and acoustic power. The former is defined in terms of the power applied to the eroded material to cause the observed pitting and volume loss. The ratio between these power quantities is termed the cavitation erosion efficiency η_{cav} and is found to be essentially constant for the range of tests, being approximately 1.4×10^{-6}. The acoustic power which is easily measured can then be used to estimate the eventual material volume erosion rates, *i.e.* the mean depth of penetration (MDPR), with much greater accuracy than is otherwise possible. The MDPR is measured directly from the weight loss and is calculated from individual pit counts on damaged surfaces. The effects of the degree of cavitation (the extent of the cavitation cloud or the cavitation number) and the throat velocity on the MDPR is examined. An overall velocity damage exponent of $n = 4.75$ is found.

1. Introduction

One of the major difficulties facing designers of liquid-flow machinery where cavitation may occur is that it is almost impossible to use feasible and practical laboratory tests to predict probable cavitation damage rates (or even their probable existence) in machines in use in the field. The development of a technique to alleviate this condition by utilizing bubble collapse pulse height spectra (PHS) obtained from microprobe transducers inserted into the cavitating region and measuring the development of damage upon specimens at an equivalent location is described. Commercially pure annealed 1100-0 aluminum was used as the test material on which individual pulses

*Presented at the International Conference on Wear of Materials, Dearborn, Mich., April 16 - 18, 1979.

from bubble collapses can most easily be registered and compared with the PHS obtained from the microtransducers. Longer tests where volume loss is inferred from weight loss are used as a measure of cavitation erosion. During the damage "incubation period" individual pit counts were used to compute the pitting deformation volume. Related work including pit counts on soft aluminum but using different flow geometries has been reported [1 - 4]. However, comparative measurements of bubble collapse PHS have only been reported from one source [5, 6].

Initial pit count deformation volumes and volume losses computed from the weight losses are presented. These were obtained upon 1100-0 aluminum specimens inserted flush with the wall of the cavitating water venturi at the same axial position as that of a Kistler microtransducer. These present essentially identical surfaces to the flow. The bubble collapse pressure pulse height acoustic power is compared with the total pit volume measured for various cavitating flow conditions. The total accumulated pit volume per time is converted into the erosion power, *i.e.* the power expended on the aluminum surface, from details of pit formation in the 1100-0 aluminum. The ratio of erosion power to acoustic power is termed "cavitation erosion efficiency" and is of the order of 10^{-6} in these tests. These values are comparable with those previously computed from the results of vibratory tests [5, 6].

Pit volume tests upon a stronger material, 2024-T-4 aluminum, are also included for one of the flow conditions used for 1100-0 aluminum. It was found that the pitting volume rate could be predicted to within a factor of 3 if it was assumed that the pitting volume rate is inversely proportional to the ultimate resilience (UR) which is consistent with numerous previous correlations reported in the literature [7].

2. Experimental facility

Tests were performed in the high speed water cavitation tunnel [8] in a Plexiglass venturi of the geometry shown in Fig. 1. The nominal throat diameter was 0.5 in (1.25 cm). The damage specimens and the microtransducer (Kistler No. 601A, resonant frequency not less than 0.1 MHz) were located at the same axial position and mounted flush with the diffuser wall in the general region of cavitation bubble collapse. For a given throat velocity the apparent extent of the cavitating region can be varied by adjusting the downstream tank pressure. Thus the apparent collapse region can be upstream of, downstream of or directly at the specimen–probe axial position. The throat velocity was varied between 25 and 49 m s^{-1} for the tests and the degree of cavitation ranged through about 5 cm centering upon the specimen–probe position.

The test liquid was Ann Arbor tap water which was partially degassed (cold-water vacuum deaerator) to 1.5% by volume (STP) as measured by a Van Slyke apparatus. The water temperature was 21 ± 2 °C.

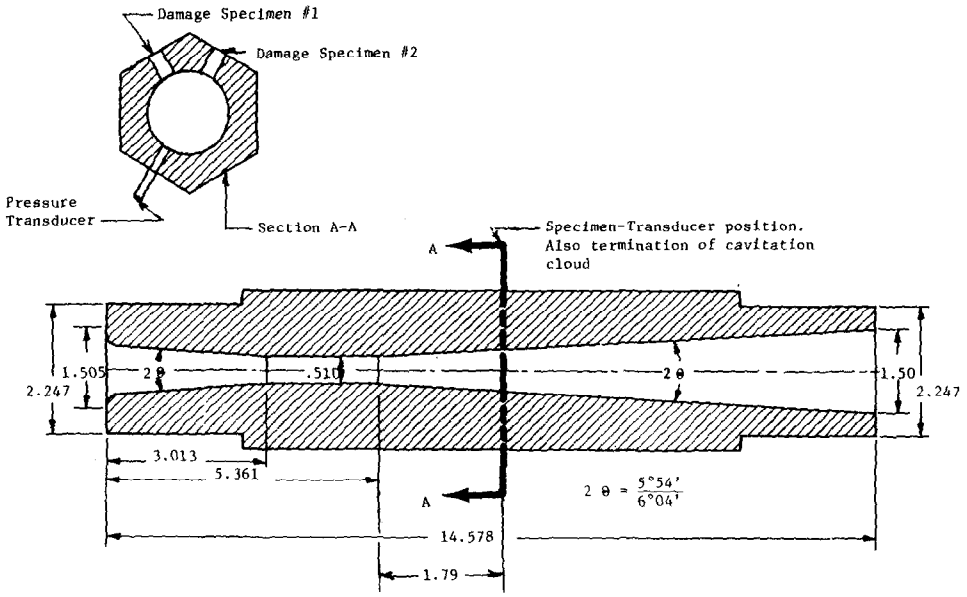

Fig. 1. Damage venturi flow path (all dimensions are in inches).

Weight loss *versus* time cavitation erosion tests were conducted with 1100-0 aluminum specimens to establish a roughly constant mean depth of penetration rate (MDPR), *i.e.* the volume loss rate per exposed area, after an initial unsteady incubation period for a throat velocity of 49 m s^{-1} and cavitation termination at the specimen–probe plane and to determine the degree of axial symmetry between the two specimen positions (Fig. 1). The effect of the test specimen geometry was also determined, *i.e.* flat end *versus* end curved to fit flush with the venturi wall. Table 1 shows that there is no systematic difference (about 10% standard deviation) in the measured $MDPR_{steady}$ as a result of either the angular position of the specimen (Fig. 1) or the end geometry. Hence the simpler flat-ended specimens could be used. Table 1 indicates a more rapid initial erosion rate for the flat-ended (non-flush) specimens. However, this end geometry more closely approximates that of the transducer.

3. Experimental results

3.1. Weight loss tests

Figure 2 [9] shows the weight loss *versus* time for 1100-0 aluminum specimens located at either position 1 or position 2 (sketch in Fig. 1) which are both axial positions where cavitation visually terminates. The maximum duration of the tests was 2 h and the specimens were weighed every 15 min. In all cases there is an initial jump in weight loss with a value of MDPR much greater than the later steady rate. The steady rates are roughly the same in all cases (Table 1) being about 4 μm h^{-1}.

TABLE 1

Cavitating venturi volume loss for 1100-0 aluminum

Specimen type	Specimen position[a]	Throat velocity ($m\ s^{-1}$)	$MDPR_{steady}$ ($\mu m\ h^{-1}$)	Initial MDP[b] (μm)
Flat	#1	49	4.667	16.312
Flat	#2	49	3.884	54.763
Flush	#1	49	4.661	25.63
Flush	#2	49	3.884	145.64

Average $MDPR_{steady}$, 4.272 $\mu m\ h^{-1}$
Standard deviation, 10.5%
Average initial MDP, 60.586 $\mu m\ h^{-1}$
Standard deviation, 97.4%

The cavitation cloud extends to the plane of the specimen.
[a]See Fig. 1.
[b]Initial MDP is calculated using data obtained after the first 30 min period.

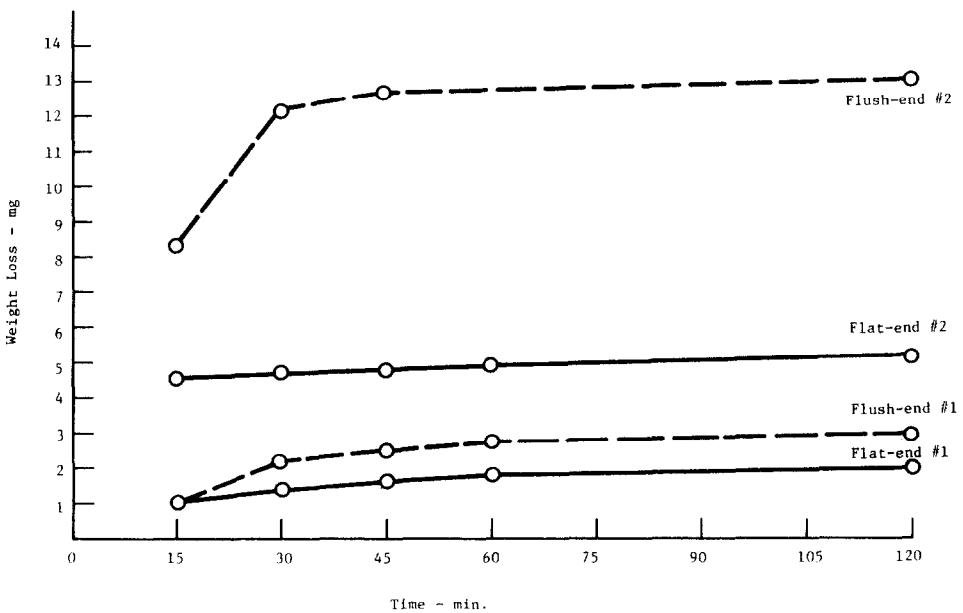

Fig. 2. Venturi weight loss for 1100-0 aluminum: broken curve, flush-ended specimen; solid curve, flat-ended specimen.

The initial jump persists through the first 30 min for the curved specimen (position 2) which indicates that it is not a result of the experimental procedure alone but rather appears to be a legitimate feature of the incubation period. While this initial surge is as yet unexplained, it is consistent with previous tests on 304 SS material using the same overall venturi geometry but an entirely different specimen design [10, 11]. One of these tests [10]

used pit count loss determination, but the initial surge was confirmed by filtering and counting radioactive debris from irradiated specimens [11]. It was then assumed that the loss of surface weak spots such as inclusions or other defects must be responsible. In the present tests the initial 15 min was investigated more closely and this will also be done in future work.

The steady weight loss results produced an MDPR of about 4 μm h^{-1} while the pitting volume calculations for the first 15 min under the same flow conditions produced a value of $MDPR_{pit}$ of 6 μm h^{-1}, *i.e.* the pit volume formed per area per unit time (Fig. 3, to be discussed later). $MDPR_{pit}$ is the value of MDPR for the total pit volume rather than for the volume loss.

The incubation period is usually assumed to consist of the formation of individual pits with little or no volume loss. In any case the loss is much less than that attained in the later "steady" period. This is clearly not the case for the present results (Fig. 2) which can be explained if the initial surges (Fig. 2) are assumed to be due to the loss of individual large surface defects or inclusions [10, 11]. These are not included in the pit counts which do not cover the entire surface but only small "typical" areas.

3.2. Pit deformation volume

The total pit volume generated on specimens exposed for 15 min under different cavitation conditions was determined by counting the individual pits and sorting them according to size. A uniform pit depth to diameter ratio of 0.1 based on previous profile traces of individual pits [12] was assumed. Optical depth determinations have been made [1, 2, 13] but the assumed uniform value of 0.1 was adequate for the present work.

The total volume of pitting was computed by assuming that the pits were spheroidal segments with a depth to diameter ratio of 0.1. The pit volume generation rate per exposed area computed during the incubation period is slightly greater than the steady weight loss MDPR, but is an order of magnitude less than the surge MDPR found during the incubation period (Fig. 2). Since the total pit volume generated should be much greater than the actual volume loss from this source [14], the discrepancy between the incubation period MDPR estimated from pit counts and that measured by weight loss is at least an order of magnitude. Thus the hypothesis that the observed weight loss surges are caused by the removal of discrete surface defects appears to be justified.

Figure 3 shows the effect that varying the degree of cavitation, *i.e.* the termination plane, has on $MDPR_{pit}$ for three throat velocities (25, 34 and 49 m s^{-1}) for runs of 15 min duration. The PHS acoustic power (in watts) is also shown for the same conditions. The shapes of the acoustic power and $MDPR_{pit}$ curves (proportional to erosion power) are nearly identical.

The presence of a maximum erosion rate cavitation "degree" (termination point) for any "intensity", *i.e.* throat velocity, where "degree" and "intensity" have their usual meanings in cavitation terminology [15], is also of interest. The maximum erosion rate is found (Fig. 3) when the cavitation termination coincides with the specimen position.

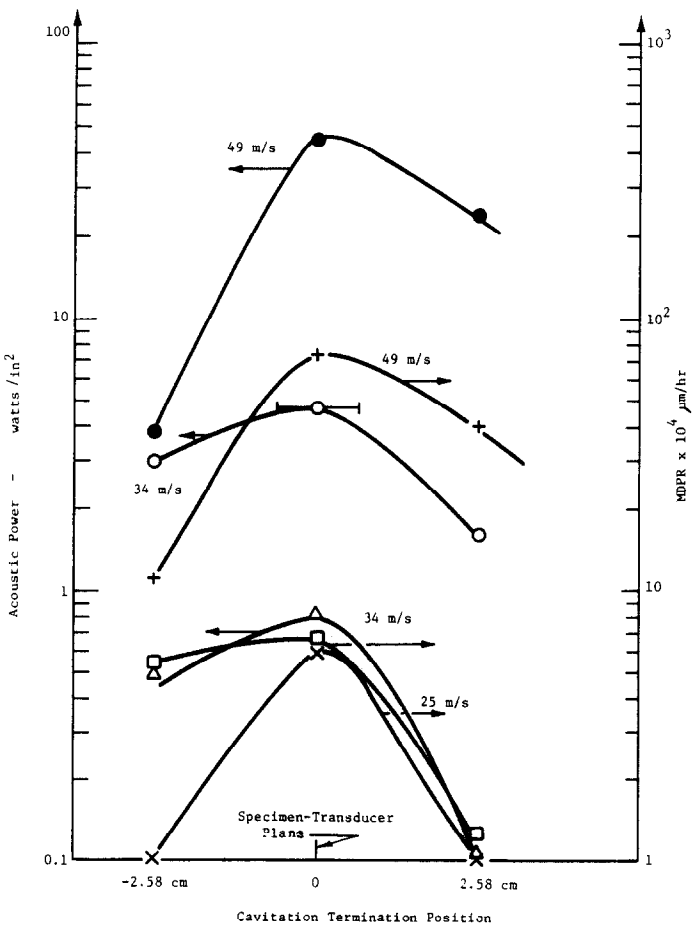

Fig. 3. Acoustic power and MDPR *vs.* extent of cavitation and throat velocity for 1100-0 aluminum.

It is found in most cases [15] that the damage rate increases with velocity. As suggested by Knapp [15] this relation is often expressed in terms of the velocity exponent n in the equation

$$\mathrm{MDPR}_1/\mathrm{MDPR}_2 = (V_1/V_2)^n \tag{1}$$

This exponent which usually has a value of about 6 [15] can vary widely [4, 15] in the present case depending on the portion of the cavitation degree curve and the velocity range (Fig. 3) considered. If the maximum degree points at the velocity extremes (25 and 49 m s^{-1} are compared $n = 4.75$ is obtained which is reasonably typical. However, in the velocity range 25 - 34 m s^{-1} n is less than unity which is not typical but is consistent with previous work [10, 14].

The similarity in the shapes of the PHS, the PHS acoustic power and the pitting volume rate (or the volume loss rate which is assumed to be pro-

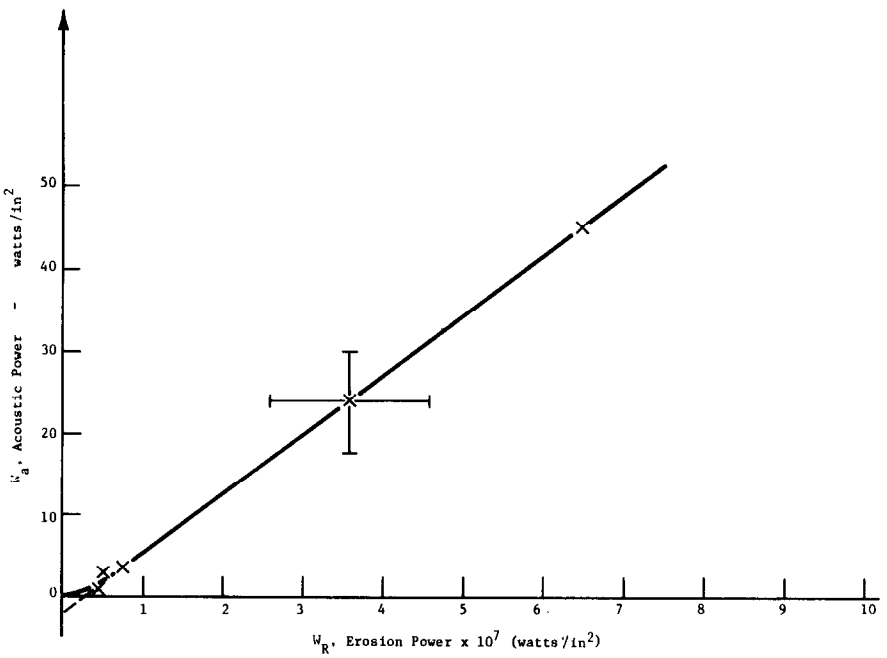

Fig. 4. Acoustic power *vs.* erosion power for 1100-0 aluminum in venturi geometry: W_R, acoustic power; W_a, erosion power.

portional to the pitting volume rate) obtained from an acoustic power PHS measurement is verified in Fig. 4 where the PHS acoustic power is plotted against the erosion power which is proportional to the pitting volume or the actual volume loss.* An excellent linear relation except for some expected threshold effects is found.

Data points for all cavitation degrees and intensities are included wherever the pertinent data were available. The full data sheets and reductions are given elsewhere [16, 17]. In the present incomplete state of this work the actual data errors are not known. A relatively large scatter bar is shown (Fig. 4) to indicate the possibility of substantial error. However, the actual data available indicate that the relation is linear with a small negative acoustic power threshold. A similar relation was postulated earlier [10] but with a positive damage threshold energy. The present negative threshold (Fig. 4) appears to indicate that the threshold for pitting of 1100-0 aluminum is less than the threshold for the present PHS circuitry, which is not surprising for the preliminary results. Presumably tests with more resistant materials will show both a positive acoustic power threshold and an increased gradient.

*The relation between the actual volume loss and the pit volume is not known, although some pertinent studies have been made [14] for other materials. No doubt it depends upon cavitation intensity and the material eroded. High intensity loading on a weak material may give both "splash" and "wash-out" [14].

TABLE 2

Comparison of 1100-0 and 2024-T-4 aluminum tests in venturi geometry

	1100-0		2024-T-4
Mechanical properties[a]			
Yield strength (lbf in^{-2})	3.5×10^3		40×10^3
Tensile strength (TS) (lbf in^{-2})	11×10^3		60×10^3
$(TS)^2/2E$ (lbf in^{-2})	6.05		180
UR_{2024}/UR_{1100} (lbf in^{-2})		$29.75 \approx 30$	
Test results			
Specimen no.	4		11
Maximum no. of pits	200 @ 0.4 mil		70 @ 0.2 mil
PHS ((lbf in^{-2}) min^{-1} in^{-2})	6.6×10^8		2.7×10^8
$A/MDPR_{pit}$ (mil/15 min)	7.19×10^{-5}		6.57×10^{-6}
$A_{1100\text{-}0}/A_{2024}$		10.94	
Conclusions			
(1) $UR_{2024}/UR_{1100} = 29.75 \approx 30$			
(2) $MDPR_{1100}/MDPR_{2024} = 10.94$			
(3) If MDPR $\propto$ 1/UR, then the cavitation intensity for the 2024 test is 30/10.94 = 2.74 times that for 1100-0			

[a]Values from Alcoa Structural Handbook

3.3. Aluminum alloy and pitting characteristics

No comprehensive tests are yet available concerning material effects on the PHS acoustic power threshold and the proportionality constant relating the acoustic power and the pitting volume rate. However, a single-point comparison [17] has been made between aluminum 1100-0 and aluminum 2024-T-4. Table 2 lists the pertinent mechanical properties and cavitation test results. As expected the average pit size is reduced and the pit number–size distribution is reduced for the stronger material [17]. $MDPR_{pit}$ is reduced by a factor of about 11. The mechanical property which shows the best linear correlation with reciprocal MDPR is generally assumed to be UR [7, 18, 19]. Since the ratio of UR values for 2024-T-4 and 1100-0 is about 30 (Table 2) the error between the UR prediction and the experimental $MDPR_{pit}$ is 30/11 = 2.7. Such a discrepancy is of the order usually expected in cavitation erosion tests [7, 19].

3.4. PHS acoustic power calculation

The energy stored in an elastic medium is proportional to the square of the pressure P since the displacement itself is proportional to P. A classical treatment of acoustic power from a point source [20] using the linear approximation gives the following relation:

$$W(R) = \frac{\text{area}}{\rho_0 C_0} \int_{t(R)}^{\tau(R)} P^2 \, dt \tag{2}$$

where $W(R)$ is the acoustic power radiated in the fluid at a distance R from the source and ρ_0 and C_0 are the density and the sonic velocity in the undisturbed liquid. $\tau(R) - t(R)$ is the pulse length which is of magnitude P. In the present tests the pulse heights P which are very short are measured by a microtransducer and a charge amplifier and recorded as oscillograms. For each pulse the integral in eqn. (2) is evaluated by assuming a square pulse of duration 2 μs. This short duration is taken from the results of Kling and Hammitt [21] who used 10^6 Hz cinematography to study bubble collapse in a similar venturi geometry. The microtransducer does not provide accurate pulse duration data since its resonant period is about 10 μs. The oscillograms were reduced manually as no suitable multichannel analyser and pulse-shaper circuitry were available.

The oscillograms provide direct PHS data (Fig. 5) which are converted to differential PHS (Fig. 6). The integral distributions

$$N(P) = \int_P^\infty N(P)\,\mathrm{d}p$$

are converted to distributions in P^2, *i.e.*

$$N(P^2) = \int_P^\infty N(P^2)\,\mathrm{d}P$$

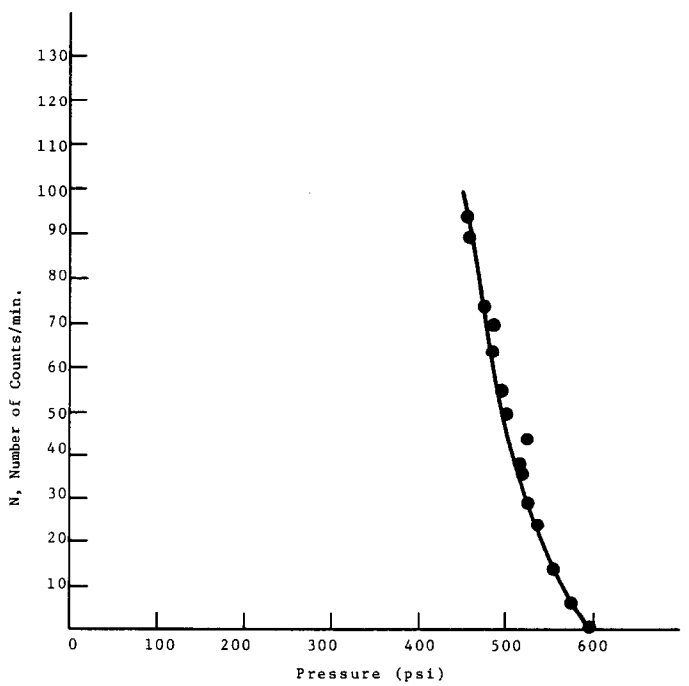

Fig. 5. Number of counts per minute *vs.* pressure for specimen no. 11 in venturi geometry with a throat velocity of 49 m s^{-1}.

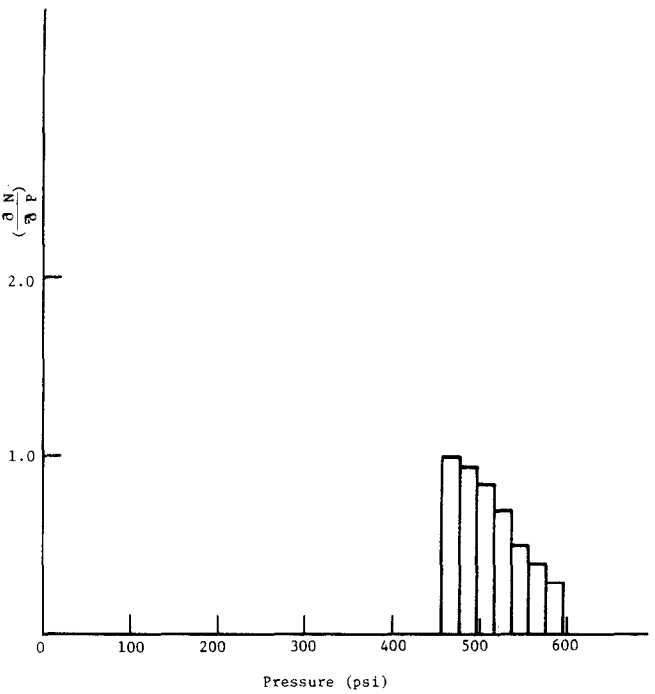

Fig. 6. Differential pressure pulse height distribution for specimen no. 11 in venturi geometry with a throat velocity of 49 m s^{-1}.

Figure 7 is a typical example but the full results are given elsewhere [16, 17]. The areas under these P^2 curves (Fig. 7) are proportional to acoustic power (eqn. (2)). The PHS acoustic power (in watts) is computed for each cavitation run for which PHS and pitting rate data had been taken. These points form the basis for Figs. 3 and 4.

3.5. Erosion power — pit volume generation and MDPR

Erosion power (in watts) corresponding to a given pit volume generation can be computed directly from the mechanical properties of the material. It has also been measured using the impact and rebound of a small steel ball on 1100-0 aluminum [1, 2, 13] which produces a value of 0.5 J mm^{-3}. This experimental value was used because the calculation of pit-forming power from $\int P$ d(vol) is uncertain. The precise pit shapes and accurate mechanical properties are unknown for such rapid loadings (compared with standard laboratory tensile tests). Also the deformation is substantially plastic so that an elastic analysis is not appropriate. It was found that $\int P$ d(vol) seriously underestimates the pitting energy, even if it is assumed that the effective value of P throughout pit formation is a factor of about 1.5 more than the handbook tensile strength of aluminum 1100-0. Therefore we preferred to use the experimental value of 0.5 J mm^{-3}. $MDPR_{pit}$ can be computed from the calculations of pit volume per exposed area and directly

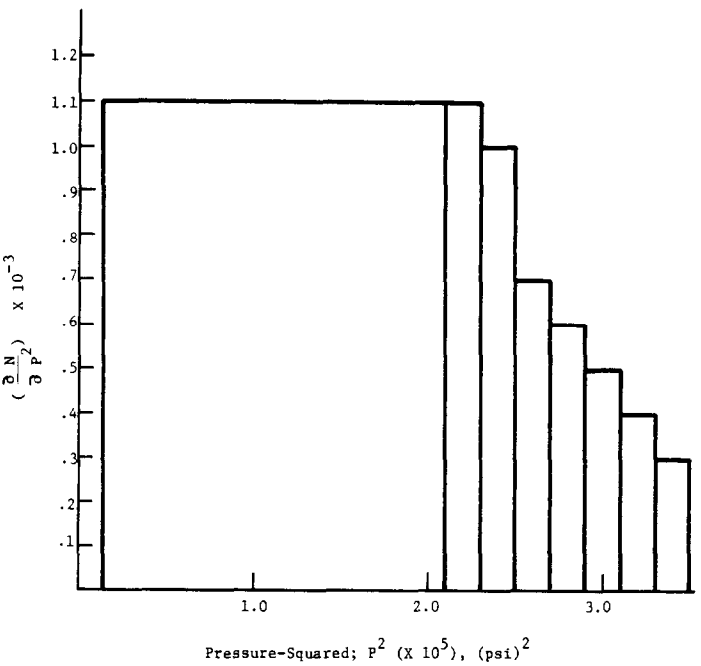

Fig. 7. Differential pressure-squared pulse height distribution for specimen no. 11 in venturi geometry with a throat velocity of 49 m s^{-1}.

related to the pitting or erosion power from the value of the energy per pit volume obtained for the aluminium 1100-0 tested.

3.6. Cavitation erosion efficiency η_{cav}

The cavitation erosion efficiency η_{cav} is the ratio of erosion or pitting-volume power to PHS acoustic power. It is computed from the linear relation of Fig. 4 as

$$\eta_{cav} = 1.44 \times 10^{-6}$$

This is a factor of about 10 greater than the values previously computed from vibratory cavitation erosion tests [5, 6] using entirely different procedures and instrumentation. A difference of 10 in a factor of 10^6 is not surprising and no comparative values exist in the literature.

Ideally η_{cav} should reflect only the ratio between the pressure energy in the liquid adjacent to the damaged material and that energy absorbed in the material which results in damage. Thus the ratio of the reflected to the absorbed energy which is primarily a function of the acoustic impedance ratio between the liquid and the sample material is involved. However, an even larger factor is that the highly loaded specimen area (pit) is much smaller than the active face of the transducer (about 5 mm). Bubble collapse photographs obtained by Kling and Hammitt [21] indicate that the impinging microjet diameter is about 10 μm. Thus the geometrical factor included in

η_{cav} could be about 0.5×10^{-6}, but its value is uncertain as is the actual ratio of reflected to absorbed energy. However, for the prediction of eventual cavitation damage rates from PHS acoustic power measurements it is not necessary to compute these factors accurately but merely to calibrate the device, assuming that η_{cav} is roughly independent of the material tested and the detailed flow conditions. Figure 4 verifies this point concerning flow conditions but gives no information on the dependence on material properties since only aluminum 1100-0 was tested.

The erosion power is actually the pitting volume power and can be related to $MDPR_{pit}$ through either the mechanical properties of the test material or the experimentally determined energy required per volume to form a pit. It should be emphasized that $MDPR_{pit}$ and MDPR (based on actual volume removed) are certainly not numerically identical and could differ substantially. However, the values of MDPR measured in the weight loss tests (about 4 μm h^{-1}) and $MDPR_{pit}$ obtained from pit volume calculations (about 6 μm h^{-1}) do not differ sufficiently for the given flow conditions for this factor to have an important effect on the magnitude of η_{cav}.

4. Conclusions

The following conclusions can be drawn from this work.

(1) The relation between PHS acoustic power and MDPR for 1100-0 aluminum in a cavitating venturi is essentially linear with a small threshold effect.

(2) The cavitation erosion efficiency η_{cav} is essentially constant (except for the threshold region) for these conditions. Its magnitude is $\eta_{cav} = 1.44 \times 10^{-6}$ for the tests described here. This value can be used for estimating MDPR from PHS acoustic power for other flow conditions and geometries.

(3) The cavitation erosion power for the tests ranges from 5×10^{-8} to 65×10^{-8} W in^{-2} (0.8×10^{-10} - 10^{-10} W mm^{-2}).

(4) The MDPR for 2024-T-4 aluminum can be predicted from the 1100-0 aluminum tests to within a factor of less than 3 by assuming that the reciprocal MDPR is proportional to UR. This UR–MDPR correlation is currently the most widely accepted correlation between mechanical properties and cavitation erosion.

(5) As expected the pit number–size spectrum for a stronger material shifts toward smaller average pit sizes and fewer pits.

(6) The maximum MDPR occurs when visual termination of the venturi cavitation cloud corresponds to the axial position of specimen damage, with reduced MDPR for either an increased or decreased cavitating region at a fixed throat velocity. This result can be interpreted in terms of varying cavitation number.

(7) The overall velocity damage exponent for the tests is $n = 4.75$, but $n < 1$ for the low velocity range.

(8) A large initial surge in MDPR (first 15 min) has been observed in weight loss tests of 1100-0 aluminum before a relatively steady value is reached. This cannot be accounted for by pit count volumes of typical specimen areas during this incubation period but is consistent with previous work using 304 SS material. The best explanation appears to be the loss of large individual surface inclusions or other defects.

Acknowledgments

This work was supported financially by the Office of Naval Research Contract No. N00014-76-C-0697 and internal University of Michigan (SEP) funds. Students assisting in the test operation and data reduction were J. Costakis, P. Felbeck, M. Grunthaner, G. Higman, T. Helmholdt and K. Kwok

References

1 D. R. Stinebring, R. E. A. Arndt and J. W. Holl, Scaling of cavitation damage, Tech. Memo Rep. No. TM 76-51, Applied Research Lab., Penn State Univ., Pa., Feb. 17, 1977.
2 D. R. Stinebring, R. E. A. Arndt and J. W. Holl, Scaling of cavitation damage, J. Hydronaut., 11 (1977) 67 - 73.
3 S. P. Hutton and J. Lobo Guerrero, The damage capacity of some cavitating flows, Proc. 5th Conf. on Fluid Machinery, Budapest, 1975.
4 H. Kato, T. Maeda and A. Magaino, Mechanism and scaling of cavitation erosion, Project Rep., Dept. of Naval Architecture, Univ. Tokyo, Bunkyo-ku, Tokyo, Japan, 1978.
5 F. G. Hammitt, S. A. Barber, M. K. De and A. N. El Hasrouni, Predictive capability for cavitation damage from bubble collapse pulse count spectra, Proc. Conf. on Scaling Performance Prediction in Rotodynamic Machines, Stirling, Sept. 6 - 8, 1977, Inst. Mech. Eng., London.
6 F. G. Hammitt, S. A. Barber, M. K. De and A. N. El Hasrouni, Cavitation damage prediction from bubble collapse pulse count spectra, Cavitation and Polyphase Flow Forum, June 1977.
7 F. G. Hammitt, Y. C. Huang, C. L. Kling, T. M. Mitchell and L. P. Solomon, A statistically verified model for correlating volume loss due to cavitation or liquid impingement, Am. Soc. Test. Mater. Spec. Tech. Publ., 474 (1969) 288.
8 F. G. Hammitt, Cavitation damage and performance research facilities, Symp. on Cavitation Research Facilities and Techniques, ASME, New York, 1964, pp. 175 - 184.
9 T. D. Helmholdt and K. H. Kwok, Cavitating venturi weight loss runs on 1100-0 aluminum, UMICH 014456-33-I, ME 490 Term Paper, Univ. Michigan, Ann Arbor, July 1978.
10 F. G. Hammitt, Observations on cavitation damage in flowing systems, J. Basic Eng., 85 (1963) 347 - 359.
11 W. J. Walsh and F. G. Hammitt, Cavitation and erosion damage measurements with radioisotopes, Nucl. Sci. Eng., 14 (1962) 217 - 223.
12 M. J. Robinson and F. G. Hammitt, Detailed damage characteristics in a cavitating venturi, J. Basic Eng., 89 (1967) 161 - 173.
13 D. R. Stinebring, J. W. Holl and R. E. A. Arndt, Two aspects of cavitation damage in the incubation zone: scaling by energy considerations and leading edge damage, International Association for Hydraulic Research Proc., Vol. 2, June 1978, Fort Collins, Colorado, pp. 463 - 477.

14 F. G. Hammitt, L. L. Barinka, M. J. Robinson, R. D. Pehlke and C. A. Siebert, Initial phase of damage to test specimens in a cavitating venturi as affected by fluid and material properties and degree of cavitation, J. Basic Eng., 87 (June 1965) 453 - 464.
15 R. T. Knapp, J. W. Daily and F. G. Hammitt, Cavitation, McGraw-Hill, New York, 1970.
16 J. S. Costakis, Cavitation effects on annealed aluminum 1100-0 for various cavitation conditions (throat velocity = 110 f/s), UMICH Project Rep. 014456-30-I (partial fulfillment of ME 490), Univ. Michigan, Ann Arbor, May 1978.
17 P. G. Felbeck, D. Higman, M. R. Grunthaner, M. K. De and F. G. Hammitt, Cavitation pitting and weight loss of 1100-0 aluminum in cavitating venturi and correlation with pressure pulse height energy, Project Rep. UMICH 014456-32-I (partial fulfillment of ME 490), Univ. Michigan, Ann Arbor, July 1978.
18 J. M. Hobbs, Experience with a 20 kc cavitation erosion test, Am. Soc. Test. Mater. Spec. Tech. Publ., 408 (1966) 159.
19 F. G. Hammitt and F. J. Heymann, Liquid erosion failures, Metals Handbook, Vol. 10, Am. Soc. Metals, Metals Park, Ohio, 1975, pp. 160 - 167.
20 H. E. Cole, Underwater Explosions, Dover Publications, New York, 1965.
21 C. L. Kling and F. G. Hammitt, A photographic study of spark-induced cavitation bubble collapse, J. Basic Eng., 94 (1972) 825 - 833.